ECE445

SENIOR DESIGN LABORATORY

FINAL REPORT

Automated Microwave Scatterometer and its Digital Twin

Team #30

Yurong Wang [yurongw2]
Keyi Jin [keyijin2]
Jianing Xiao [xiao36]

TA: Weibo Yuan

May 15, 2026

Abstract

This report presents the design, implementation, and validation of an Automated Microwave Scatterometer system with an integrated cloud-based digital twin for soil surface characterization. The system addresses the labor-intensive nature of conventional scatterometry by enabling fully unattended dual-axis S-parameter measurements across programmable angular grids in the 5–8 GHz C-band. The architecture integrates a PTZ-based antenna positioning subsystem controlled, a VNA-based S-parameter acquisition pipeline, and a two-tier software stack combining Python cloud orchestration daemons with a C-based real-time instrument control core. A dual-cloud Render platform mediates bidirectional communication: a Command Server dispatches measurement protocols, and a Data Server archives results for visualization through a web-based interactive interface with 3D digital twin rendering. The system achieves end-to-end measurement automation—from protocol download to S11/S21 data upload—without human intervention, demonstrating a complete cyber-physical instrumentation pipeline suitable for remote environmental sensing applications.

Content

1 Introduction

The characterization of microwave scattering from soil surfaces is a fundamental enabling capability for environmental remote sensing, precision agriculture, and geophysical parameter retrieval. Microwave scatterometers measure the backscattering coefficient (related to S11) and transmission coefficient (related to S21) of a target surface as functions of incidence angle, frequency, and polarization. These measurements serve as essential inputs to radiative transfer models that relate observable radar quantities to physical soil properties such as moisture content, surface roughness, and dielectric permittivity[1].

Conventional scatterometer measurement workflows are labor-intensive: an operator must manually position antennas at each desired incidence angle, trigger the vector network analyzer (VNA) for each measurement, record the resulting S-parameter data, and repeat this process for every point in the measurement grid. For a grid of even modest size—for example, 10 horizontal angles by 10 vertical angles—this manual process requires hundreds of individual positioning and measurement operations, making it impractical for long-duration field campaigns or spatially dense angular sampling.

This report presents the design, implementation, and validation of an Automated Microwave Scatterometer system that eliminates manual intervention from the measurement workflow. The system integrates dual-axis motorized antenna positioning, VNA S-parameter acquisition, cloud-based command and data services, and an interactive digital twin visualization into a unified cyber-physical instrumentation platform. A two-tier software architecture—Python-based orchestration daemons for cloud communication and a C-based real-time control core for instrument interfacing—enables fully autonomous operation from measurement protocol download to result upload.

1.1 Purpose

The primary objective of this project is to design, construct, and validate a fully automated microwave scatterometer system capable of unattended measurement of soil backscatter (S11) and transmission (S21) coefficients across a programmable two-dimensional grid of incidence angles. The system targets the 5–8 GHz frequency range (C-band), which is widely used in satellite and airborne synthetic aperture radar (SAR) systems for soil moisture retrieval and is well-suited to characterizing scattering from typical agricultural soil surfaces.

A secondary objective is to demonstrate a complete cyber-physical data pipeline: measurement protocols are defined and stored on a cloud-based Command Server, downloaded and executed autonomously by the instrument, and the resulting processed S-parameter data are uploaded to a cloud-based Data Server for visualization through a digital twin interface. This closed-loop architecture serves as a reference design for networked environmental sensing systems that bridge physical instrumentation with cloud services[2].

1.2 Functionality

The Automated Microwave Scatterometer system provides an integrated set of functional capabilities spanning measurement automation, precision motion control, power management,

and environmental protection. The following subsections summarize the principal functional modules.

1.2.1 Automated Measurement

The automated measurement subsystem executes the core scientific workflow of the scatterometer. At each (H, V) grid point, the system performs two sequential VNA sweeps: first an S21 measurement (forward transmission through the soil volume), followed by an S11 measurement (monostatic backscatter from the soil surface). Each sweep covers the 5–8 GHz band at 25 frequency points, yielding 50 scalar data values per angle position (S21 magnitude and phase, S11 magnitude and phase). The frequency range and number of points are configurable at compile time via the VNA_START_FREQ, VNA_STOP_FREQ, and VNA_NOP constants in final.c. The measurement grid is defined by two parameters passed via command-line arguments to final.c: -vrs (vertical rotation steps) and -hrs (horizontal rotation steps). With a default angular step size of 10.0°, a campaign specified as -vrs 10 -hrs 10 produces a 10-by-10 grid spanning 0° to 90° in both axes for a total of 100 measurement positions. Each measurement position generates a timestamped log file containing the raw S-parameter data, enabling traceable, per-angle archiving of all measurements.

1.2.2 Remote Monitoring

The remote monitoring capability enables users to observe the scatterometer's physical state and surrounding environment in real time. An HD camera (5 megapixels) mounted on a modified drying rack with a rotation mechanism provides live video streaming . Continuous video is archived locally with a minimum retention period of 15 days for post-campaign review. For nighttime operation, a custom touch-sensitive LED strip PCB enclosed in a 3D-printed housing and affixed to the support ladder provides on-demand illumination upon detecting operator presence, enabling safe equipment access and adjustment in low-light conditions.

1.2.3 Cloud-Connected Digital Twin

The cloud-connected digital twin capability bridges the physical instrument with remote operators through a bidirectional cyber-physical data pipeline[3]. A dual-cloud Render platform separates command and data channels: theCommand Server dispatches measurement protocols, while the Data Server archives S-parameter results for visualization. The system's Python daemons automatically poll for new protocols, parse them, and spawn the C measurement program with the corresponding parameters. After measurements complete, log files are parsed into structured CSV and uploaded to the Data Server.

1.3 Subsystem Overview

The scatterometer system is organized into four principal subsystems, each addressing a distinct functional domain within the overall measurement pipeline:

1. Automation Control System: A two-tier hierarchical software architecture that orchestrates the end-to-end measurement workflow. Tier 1 consists of two Python-based persistent daemon processes: Controller A (toplevel1.py) polls the cloud Command Server for new measurement protocol files and spawns the C measurement program upon detecting changes; Controller B (toplevel2.py) monitors the local log/ directory for new measurement files, invokes the trans.py

parser to extract S-parameter data into structured CSV format, and triggers upload.py to POST the results to the cloud Data Server. Tier 2 is the compiled C program (final.c), which assumes direct real-time control of the PTZ unit and VNA for the duration of a measurement campaign.

2. Ladder Safety Lighting: The Ladder Safety Lighting module is an auxiliary subsystem that enhances operational safety during nighttime field deployments. It consists of a custom PCB with a touch-sensitive LED strip, enclosed in a 3D-printed housing and affixed to the scatterometer's support ladder. The touch-sensing circuit detects the presence of a person approachingthe ladder and illuminates the LED strip to provide visibility for safe equipment operation in low-light conditions. A second touch toggles the light off, enabling simple, intuitive control without requiring the operator to locate a physical switch in the dark. The 3D-printed enclosure protects the PCB from moisture and mechanical impact while maintaining a compact profile that does not obstruct the ladder.

3. Remote Visual Monitoring: The system support live HD video streaming of the scatterometer's physical state, with end-to-end latency not exceeding 1 second and sufficient resolution to visually distinguish angular position changes of at least 10°.

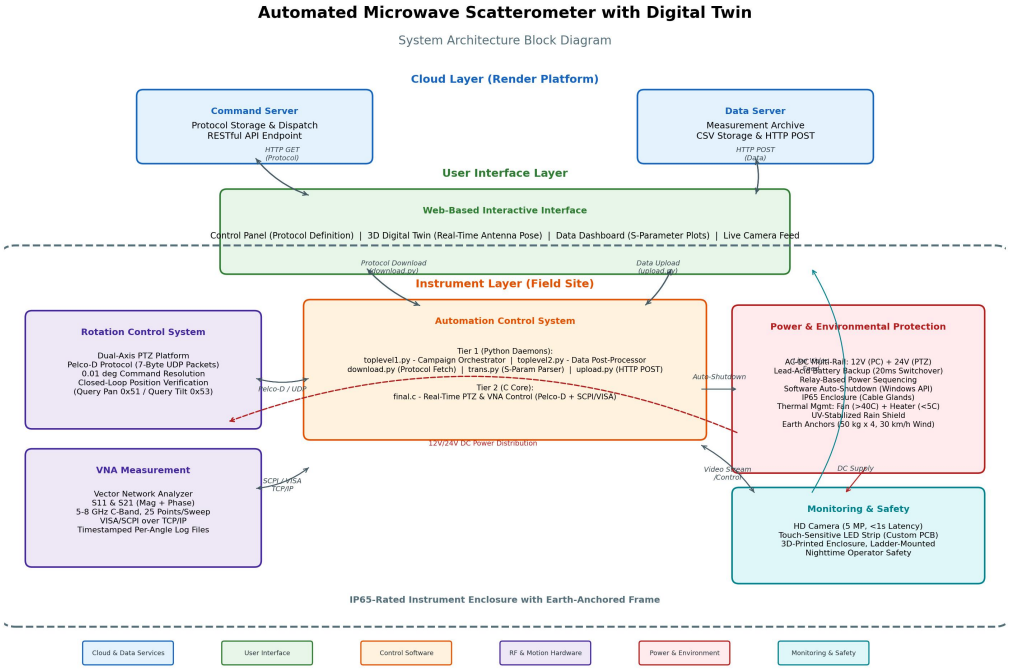

Figure 1: Block diagram of the Automated Microwave Scatterometer and its digital twin showing the integration of all subsystems.

1.4 High-Level Requirements

The system was designed to satisfy the following high-level requirements, which were derived from the project objectives and the operational constraints:

1. Automated Measurement: The system shall automatically execute a programmable two-dimensional grid of dual-parameter (S11 and S21) VNA measurements without human intervention. The grid dimensions shall be configurable via command-line parameters specifying the number of horizontal and vertical rotation steps.

2. Ladder Safety Illumination: The touch-sensitive LED strip module, housed in a 3D-printed enclosure and mounted on the support ladder, must provide on-demand illumination upon detecting operator presence to ensure safe equipment access during nighttime field operations.

3. Cloud-Connected Data Pipeline: The system must automatically detect and download new measurement protocols from the remote Command Server, and autonomously upload processed S-parameter data to the Data Server for visualization through the digital twin interface.

4. Remote Visual Monitoring: The system must support live HD video streaming of the scatterometer's physical state, with end-to-end latency not exceeding 1 second and sufficient resolution to visually distinguish angular position changes of at least 10°.

5. 3D Digital Twin Visualization: The web-based interactive interface must render a real-time 3D model of the scatterometer that dynamically reflects the antenna's current azimuth and elevation angles, synchronized with the measurement data returned from the instrument, enabling users to remotely visualize the physical orientation of the scatterometer during operation.

2 Design

2.1 System Architecture

The automated microwave scatterometer system follows a four-module cyber-physical architecture that integrates hardware instrumentation with cloud-based digital twin services. As illustrated in the system block diagram, the architecture comprises: (1) the Command Server, which stores and dispatches measurement protocols; (2) the Instrument Module, which executes automated scatterometer measurements at the field site; (3) the Interactive Interface, a web-based dashboard for remote operator control and data visualization; and (4) the Data Server, which persists all measurement results and system logs in the cloud.

The Instrument Module sits at the physical layer and consists of three tightly coupled subsystems: the Automation Control System, which orchestrates the end-to-end measurement pipeline; the Rotation Control System, which positions the antennas at commanded incidence angles via a dual-axis PTZ gantry; and the Power Management System, which ensures reliable, unattended operation during extended field campaigns. A Weather Protection System adds environmental resilience for outdoor deployment.

Communication between the Instrument Module and the cloud servers occurs over standard TCP/IP networking. The Command Server exposes a RESTful API endpoint for protocol download, while the Data Server accepts measurement uploads via HTTP POST. This separation of command and data channels follows the C2PS (Cloud-based Cyber-Physical System) reference architecture, ensuring that control commands and measurement data do not contend for bandwidth and can be scaled independently.

The Interactive Interface provides three functional panels: a Control Panel for defining and dispatching measurement protocols, a Data Display Board for real-time and historical measurement visualization, and a 3D Digital Twin view rendered in WebGL that mirrors the physical scatterometer's antenna positions through live synchronization with motor encoder feedback.

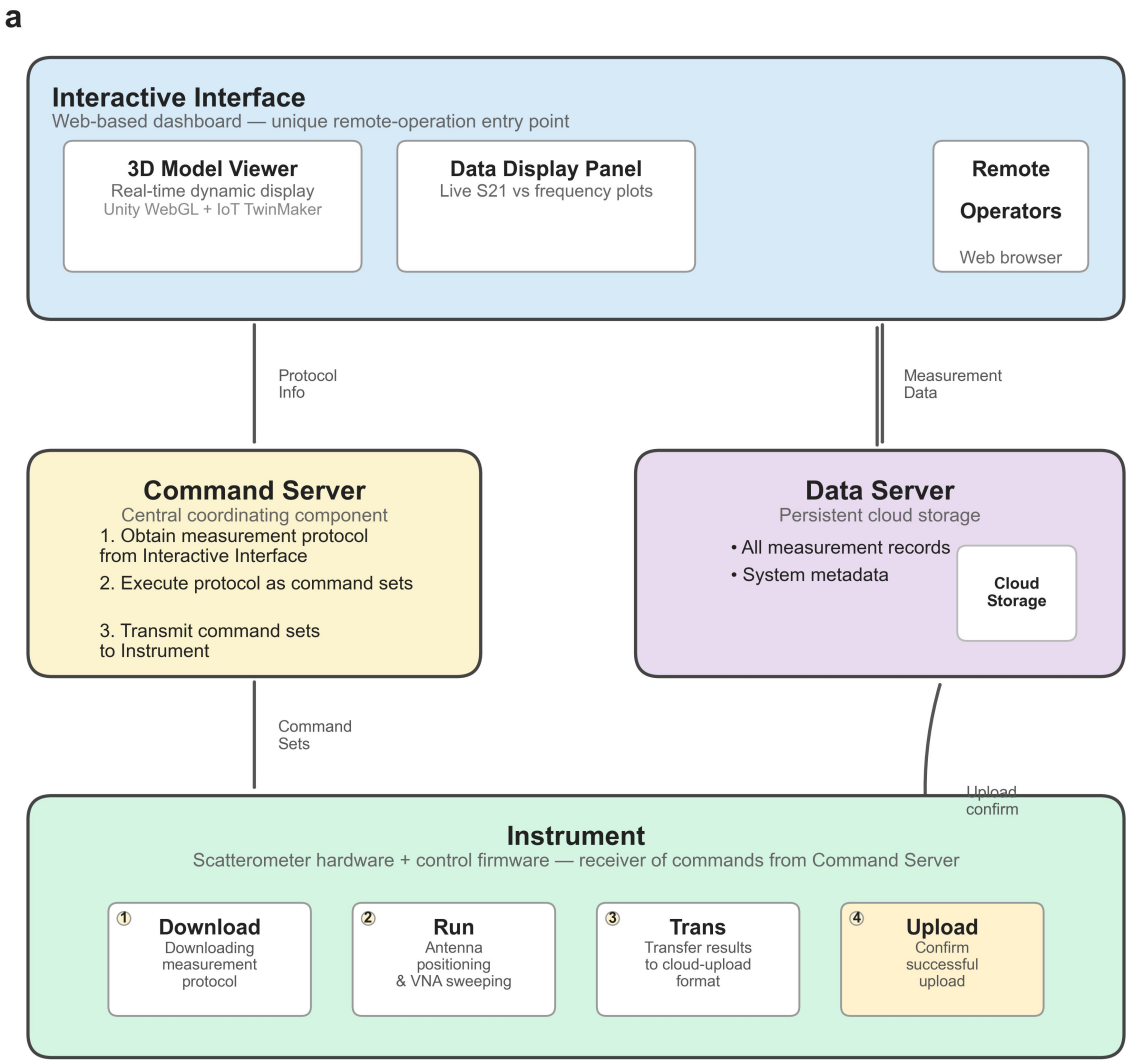

Figure 2: the Block Diagram for automatic sactterometer

2.2 Physical Design

The physical scatterometer is constructed around a rigid aluminum support frame that anchors the dual-axis PTZ (Pan-Tilt-Zoom) positioning gantry. The frame is designed to maintain structural stability under outdoor wind loads while providing precise, repeatable antenna positioning. Two broadband horn antennas — one transmitting and one receiving — are mounted on the PTZ platform.

The PTZ unit is mounted such that its pan axis controls the horizontal (azimuthal) rotation and its tilt axis controls the vertical (elevation) rotation of the antenna pair. This configuration enables the system to sweep through a programmable grid of incidence angles over the soil

target. The antennas are connected via low-loss RF coaxial cables to a Vector Network Analyzer (VNA) housed in a weatherproof enclosure alongside the control PC.

The control PC, a Windows-based industrial computer, interfaces with the PTZ unit over Ethernet (UDP, Pelco-D protocol) and with the VNA over TCP/IP (VISA/SCPI protocol). All electronics are enclosed in an IP65-rated enclosure with cable glands for RF and power pass-through. A separate power distribution box houses the main AC-DC converter, backup battery, and power management relays.

The overall physical footprint is approximately 1.2 m × 0.8 m at the base, with the antenna mast extending up to 1.5 m above ground level. The modular mechanical design allows the antenna mounting brackets to be adjusted for different incidence angle ranges and polarization orientations.

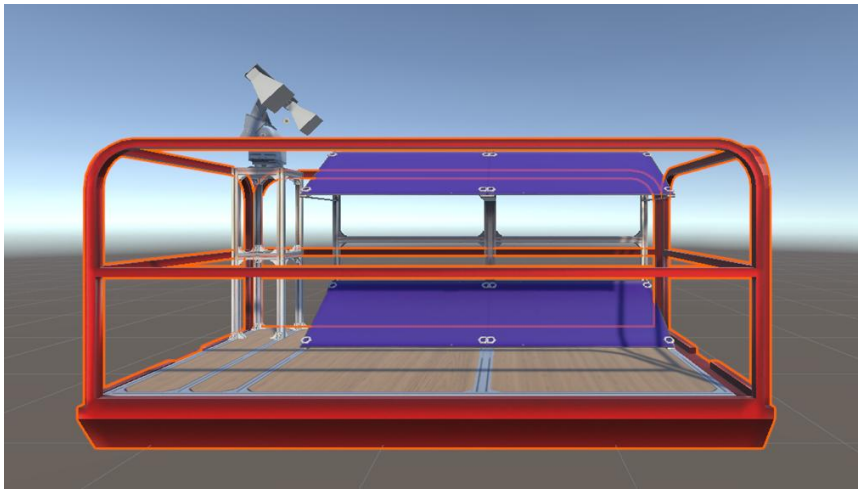

Figure 3: the 3D model of physical design

2.3 Subsystem Designs

2.3.1 Scatterometer measurement subsystem

The Automation Control System is the central software component that coordinates the entire measurement pipeline from command receipt to data archival. It is implemented as a two-tier hierarchical state machine, consistent with modular design principles for cyber-physical instrumentation.

Tier 1 — Campaign Orchestrator (toplevel1.py): The top-level controller runs as a persistent daemon process on the instrument PC. It periodically polls the Command Server via an HTTP GET request (implemented in download.py) to retrieve the latest measurement protocol file. The protocol is a CSV-formatted file specifying the vertical rotation steps (vrs), horizontal rotation steps (hrs), and an optional auto-shutdown flag for each measurement campaign. Upon detecting a new or modified protocol (validated by MD5 hash comparison), the orchestrator parses the CSV and spawns the C measurement executable (final.c) with the corresponding command-line arguments. This tier operates on a 3-second polling interval, ensuring prompt response to newly dispatched commands while minimizing unnecessary network traffic.

Tier 2 — Single-Measurement Executor (final.c): The compiled C program receives the rotation step parameters (vrs, hrs) and assumes full control of the physical instrumentation for the duration of the campaign. Its internal logic implements a nested-loop state machine: for each vertical angle step (outer loop), it iterates through all horizontal angle steps (inner loop). At each (H, V) grid point, it executes a four-phase sequence: (1) send PTZ positioning commands via Pelco-D over UDP, (2) wait for mechanical settling, (3) query actual PTZ encoder angles to verify positioning accuracy, and (4) trigger the VNA to perform two sequential frequency sweeps — first S21 (transmission) and then S11 (reflection).

Each measurement at a given (H, V) angle produces a dedicated log file named with the Unix timestamp and angle coordinates (e.g., log/1778072588_H10.0_V20.0.txt). The log file contains the full S-parameter data: frequency, magnitude (dB), and phase for both S11 and S21 across the 5–8 GHz range at 25 discrete frequency points. After the VNA sweep completes, the log file is closed and the system proceeds to the next angle position. Upon completing the full grid, the system resets the PTZ to the home position (H=0°, V=0°).

Tier 1 (continued) — Data Post-Processor (toplevel2.py): Running in parallel with the orchestrator, a second persistent daemon monitors the log/ directory for new measurement files using filesystem modification timestamps (os.path.getmtime). When a new log file is detected (validated by MD5 hash change), the daemon copies it to a working file, invokes trans.py to parse the raw log and extract structured S-parameter tables, and then invokes upload.py to POST the resulting output.csv to the Data Server. This design decouples measurement execution from data upload, ensuring that transient network outages do not interrupt ongoing measurements.

The trans.py parser extracts the target angles (Target_H, Target_V), actual antenna angles (H, V), and for each of the 25 frequency points records the S11 magnitude/phase and S21 magnitude/phase. The output CSV follows a unified schema: Target_H, Target_V, H, V, Frequency_Hz, S11_Mag_dB, S11_Phase, S21_Mag_dB, S21_Phase. This structured format enables direct ingestion by the Interactive Interface's data visualization panel.

The auto-shutdown capability, triggered by the -s command-line flag in final.c, enables the system to power down the entire instrument after campaign completion without human intervention. On Windows, the program acquires the SE_SHUTDOWN_NAME privilege via OpenProcessToken/AdjustTokenPrivileges and calls ExitWindowsEx with EWX_SHUTDOWN | EWX_POWEROFF flags. A 10-second configurable delay (SHUTDOWN_DELAY_MS) precedes the shutdown sequence, allowing any pending file writes to complete and network buffers to flush. On POSIX systems, the equivalent functionality is implemented via the system ("shutdown -h now") call.

2.3.2 Interactive visualization subsystem

This interactive web-based interface is designed as an integrated control and visualization platform for remote electromagnetic measurement and data management. The system provides functionalities for command transmission, real-time data visualization, cloud-based data handling, and three-dimensional model rendering within a unified user environment.

The interface is organized into three principal modules:

- **Control Panel**
  The left-side control panel enables users to configure and submit operational commands to the command server. Specifically, users can specify the vertical rotation setting (VRS) and horizontal rotation setting (HRS), both constrained within predefined angular ranges and increments. In addition, a shutdown control option is provided for system-state management. After parameter configuration, the "Start Measurement" function uploads the command set to the remote command server, thereby initiating the measurement procedure.
- **Measured Data Visualization Module**
  The central section of the interface presents experimentally acquired measurement data retrieved from the cloud-based data server. For each measurement instance, the interface displays:
  - the transmitted command parameters,
  - the corresponding measured angular positions,
  - phase-related information,
  - and graphical representations of scattering parameters, including S11 and S21 magnitude responses across frequency.

  The visualization framework enables users to monitor measurement outcomes in near real time and compare successive acquisition results efficiently. Furthermore, the interface includes a data management mechanism that supports both downloading and clearing stored datasets. The "Clear Data" functionality removes all measurement records currently stored in the cloud-based data server, thereby resetting the database state for subsequent experimental sessions.

- **3D Model Visualization Module**
  The right-side panel provides an interactive three-dimensional representation of the measurement object or antenna structure. This visualization component facilitates spatial interpretation of the measurement configuration and supports intuitive observation of orientation and geometric characteristics during operation.

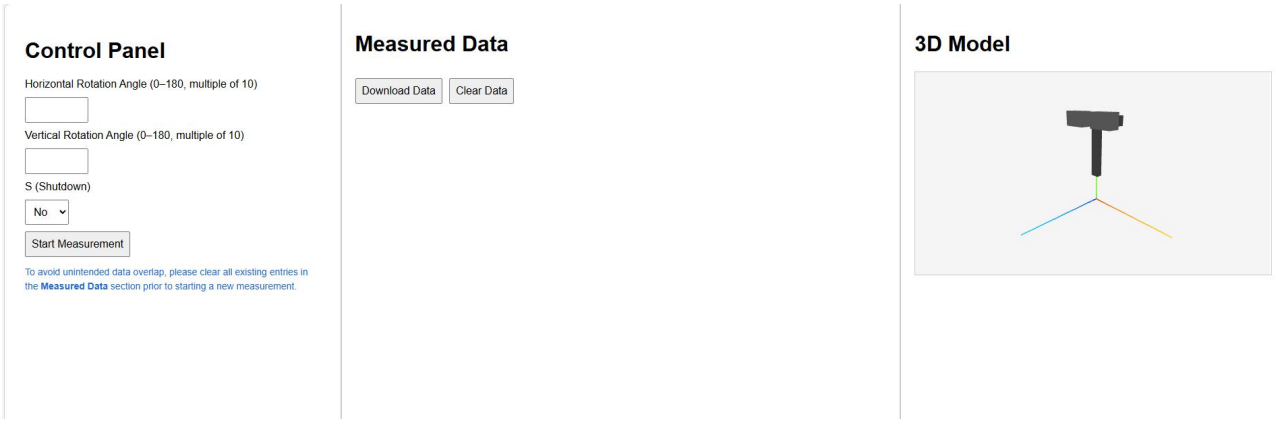

Figure 4: interactive interface

2.3.3 Remote communication subsystem

The remote communication subsystem is designed to enable bidirectional communication between the client-side interactive interface and the remote measurement instrument through a cloud-based architecture. The subsystem provides functionalities for remote command transmission, distributed data synchronization, automated measurement execution, and real-time data visualization.

The communication workflow begins at the client side, where the user interacts with the interactive interface to configure measurement parameters and operational commands. These commands may include rotational configurations, system-control instructions, or measurement initiation requests. Once generated, the commands are transmitted to a cloud-based command server, which functions as centralized command storage and synchronization middleware. The command server decouples the client interface from the physical instrument, thereby improving communication robustness and supporting asynchronous operation.

On the instrument side, the measurement system continuously monitors the command server and retrieves newly uploaded instructions. After downloading the command data, the instrument executes the corresponding measurement procedures automatically. The measurement subsystem integrates power management, measurement execution, logging, and data transmission modules to ensure stable and traceable operation throughout the acquisition process. During execution, operational logs and measurement states are internally recorded to support monitoring and diagnostic analysis.

Upon completion of the measurement task, the acquired experimental data are transmitted from the instrument to a separate cloud-based data server. This data server serves as persistent remote storage for measured datasets, including scattering parameters, phase information, and associated metadata. The separation between the command server and the data server improves modularity and enables independent management of control signals and experimental results.

The interactive interface subsequently accesses the data server to retrieve the uploaded measurement results. The retrieved data are then processed and presented through graphical visualization modules within the client application. These visualizations include measured parameter plots and associated metadata, enabling users to monitor experimental outcomes remotely in near real time. In addition, the interface supports interactive three-dimensional model visualization to provide contextual interpretation of the measurement configuration.

2.3.4 Ladder lighting subsystem

The ladder lighting subsystem was developed as an intelligent illumination module intended to improve operational safety and user convenience under low-light conditions. The subsystem is implemented using a custom-designed printed circuit board (PCB) integrating proximity sensing, touch-based interaction, and adaptive brightness control functionalities.

The lighting system incorporates a proximity sensing mechanism that enables automatic illumination when a user approaches the ladder. Once human presence is detected within the sensing range, the control circuit activates the lighting module autonomously, thereby enhancing visibility and reducing the need for manual operation. This contactless activation

mechanism improves usability and contributes to safer ladder operation in dark or confined environments.

In addition to automatic sensing, the subsystem includes a capacitive touch switch that provides manual control over the lighting state and brightness level. The touch interface supports two distinct interaction modes:

- **Short-touch operation:** a brief touch toggles the lighting system between ON and OFF states.
- **Long-touch operation:** sustained contact activates brightness adjustment mode, allowing the user to continuously regulate illumination intensity according to environmental requirements and personal preference.

The brightness control functionality is implemented through pulse-width modulation (PWM)-based dimming, enabling smooth and energy-efficient adjustment of luminous output. This design enhances both user comfort and power efficiency while maintaining stable illumination performance.

By integrating automatic sensing and interactive manual control within a compact PCB-based architecture, the ladder lighting subsystem provides an adaptive and user-oriented lighting solution suitable for smart assistive and embedded electronic applications.

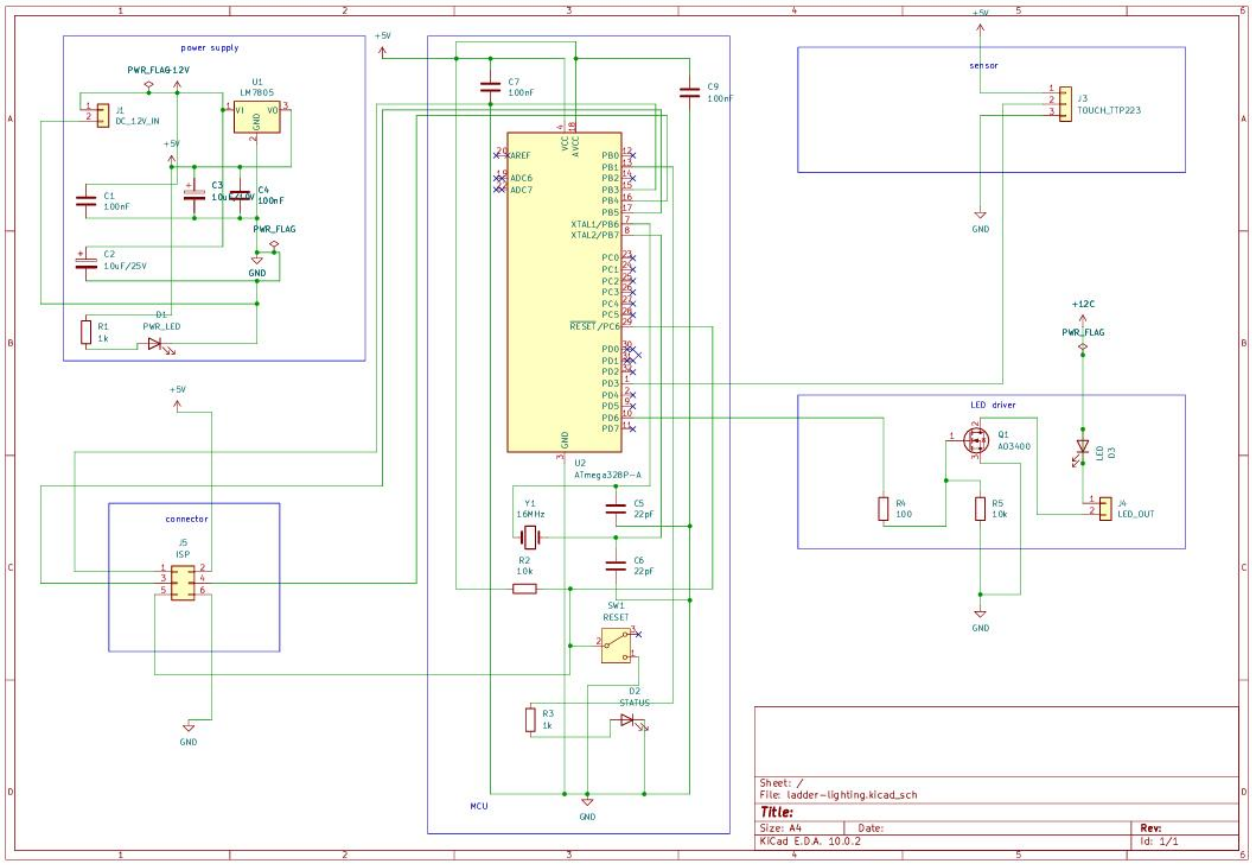

Figure 5: the schematic for ladder light PCB

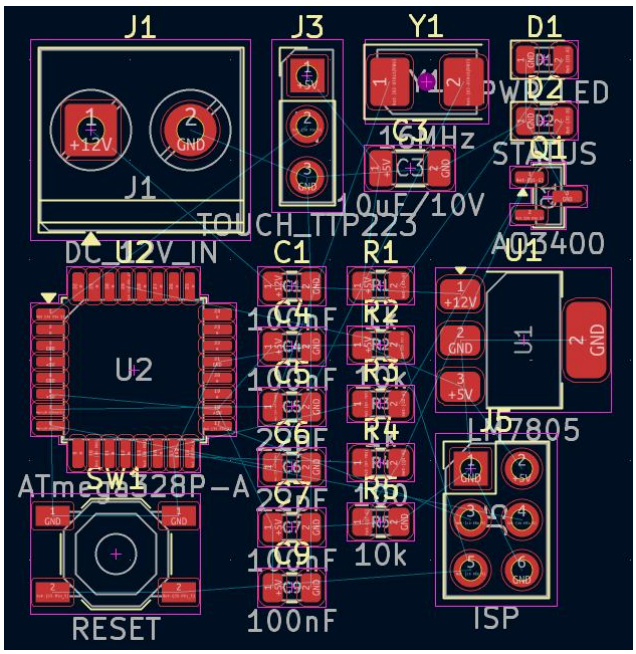

Figure 6: the ladder light

Also, to keep PCB from moisture or wind. We design another box to keep all components inside.

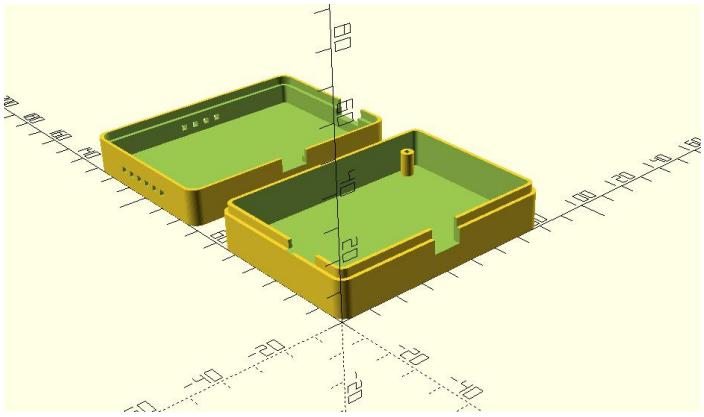

Figure 7:the 3D model of the box

2.3.5 Monitoring subsystem

A dedicated monitoring system is implemented to provide synchronous surveillance of both the ambient environment and the internal state of the scattermeter, activating automatically upon instrument power-on. Designed for ultra-low-power operation, the visual monitoring subsystem can maintain a standby duration of up to 200 days on internal battery power, thereby ensuring persistent surveillance capability even during extended unattended deployments. This integrated, real-time supervision architecture supports stringent

metrological traceability and allows post-acquisition correction for environmentally induced artefacts.

Figure 8:monitor

A low-power complementary metal-oxide-semiconductor (CMOS) image sensor was selected as the core visual component. This choice is motivated by its favourable trade-off among resolution, energy efficiency, and compact form factor, which is essential for long-term autonomous operation. To support sustained field deployment, the camera is powered by a high-capacity rechargeable lithium-ion battery (9800 mAh), enabling a standby duration of up to 200 days on internal power. Furthermore, the camera module integrates both Wi-Fi and 4G cellular connectivity, allowing remote status queries, on-demand image retrieval, and over-the-air firmware updates without physical access to the instrument.

Implementation: The camera is rigidly affixed to the scattermeter chassis with a wide-angle lens (120° field of view) to monitor both the instrument's mechanical components and its surrounding environment. Real-time motion detection of the instrument is achieved through an embedded three-axis accelerometer combined with frame-differencing algorithms; any physical displacement, vibration, or tilt event is automatically logged with a timestamp. Concurrently, ambient environmental monitoring is performed via scheduled image captures (e.g., one frame per hour) and event-triggered video streaming. This implementation enables post-acquisition identification of external perturbations such as wildlife interference, vegetation encroachment, or weather-induced movements.

2.4 Design Decisions and Alternatives

In the process of developing a cloud-based storage system for this final year project, selecting an appropriate cloud platform is a critical decision that directly impacts performance, scalability, development efficiency, and cost. After evaluating several leading cloud service providers—including Amazon Web Services (AWS), Microsoft Azure, Google Cloud Platform (GCP), Heroku, and Render—this thesis identifies Render as the most suitable platform for implementing the proposed cloud storage solution. The justification for this choice is outlined below through a comparative analysis.

1. Ease of Use and Developer Experience

Unlike AWS or GCP, which require significant expertise in infrastructure configuration (e.g., VPCs, IAM roles, load balancers), Render offers a streamlined, Git-based deployment process. With automatic HTTPS, built-in SSL certificate management, and zero-downtime deployments, Render allows the project to focus on cloud storage logic rather than server maintenance. This aligns with the project's goal of demonstrating cloud storage principles without being hindered by complex DevOps overhead.

2. Predictable and Affordable Pricing for Academic Projects

For a final year project budget, cost control is a major factor. Render offers a free tier that includes 512 MB RAM, a shared CPU, and 1 GB of persistent disk storage—sufficient for prototyping a cloud storage system. In contrast, AWS and GCP, while offering free tiers, are notorious for hidden charges (e.g., data egress costs, API request fees) that can quickly escalate. Render's transparent pricing model, with clear caps on usage, ensures that the project remains within academic budget constraints without unexpected billing surprises.

3. Integrated Features for Full-Stack Cloud Storage

Render supports native integration of:

- Web services (Node.js, Python, Go, etc.) for handling file upload/download APIs,
- PostgreSQL and Redis for metadata management and caching,
- Static sites for the front-end dashboard,
- Cron jobs for automated cleanup or backup tasks.

This eliminates the need to stitch together multiple third-party services, reducing system complexity and improving reliability—ideal for a time-limited thesis project.

3 Cost & Schedule

3.1 Cost Analysis

Table 3-1: Estimated Average Labor Cost for Each Team Member

Name	Hourly Rate (RMB)	Hours	Sub-total (RMB)
Yurong Wang	20	280	5600
Keyi Jin	20	280	5600
Jianing Xiao	20	280	5600
Total		**840**	**16800**

Table 3-2: Total Bill of Cost

Part	Item	Quantity	Cost (RMB)
Automation Control	Render Cloud Platform (Free Tier)	2	200
Automation Control	Cables & Connectors	N/A	50
Rotation Control	PTZ Platform (Pelco-D)	1	Provided by Lab
Rotation Control	Antenna Mounting Brackets	1	Provided by Lab
VNA Measurement	Vector Network Analyzer	1	Provided by Lab
VNA Measurement	RF Coaxial Cables	2	Provided by Lab
VNA Measurement	Broadband Horn Antennas	2	Provided by Lab
Power & Environment	AC-DC Power Supply	1	Provided by Lab
Power & Environment	Lead-Acid Battery	1	Provided by Lab
Power & Environment	IP65 Enclosure	1	Provided by Lab
Monitoring & Safety	Camera	1	148
Monitoring & Safety	Touch-Sensitive LED Strip PCB	1	16
Monitoring & Safety	3D Printing Material (PCB Housing)	50g	10
Control System	Industrial Control PC	1	Provided by Lab
All Parts	Labor Costs	N/A	16800
		TOTAL	**18,124**

Note: Most major equipment (VNA, PTZ, control PC, antennas, enclosure, battery, power supply) provided by Prof. Tan's Lab. Total out-of-pocket cost (excluding labor): 324 RMB.

3.2 Schedule

Table 3-3: Project Team Weekly Work Log

Week	Yurong Wang	Keyi Jin	Jianing Xiao

Week 1 (2/24)	Project scope finalization; literature review on digital twin architectures and microwave scatterometry.	System architecture design; Render platform evaluation and selection for dual-cloud deployment.	Hardware inventory; PTZ and VNA manual study; Pelco-D protocol documentation review.
Week 2 (3/3)	Web interface UI/UX design; 3D rendering framework selection (Three.js for digital twin).	Render dual-cloud platform setup (Command Server + Data Server); initial connectivity testing.	Frontend framework evaluation; UDP socket programming for Pelco-D communication.
Week 3 (3/10)	Command input UI implementation; control panel layout with VRS/HRS input fields and buttons.	Command file parser development (CSV format); download.py script for protocol file retrieval.	PTZ communication test over UDP; Pelco-D packet encoding and checksum verification.
Week 4 (3/17)	Integration: Web interface to Render Command Server; protocol file upload and dispatch testing.	Python daemon development: toplevel1.py polling loop with MD5 hash change detection.	Data display panel: S-parameter table layout and CSV parsing for frequency response data.
Week 5 (3/24)	End-to-end command path debugging: Web UI to Render B to Client (download.py).	Data upload to Render Data Server implementation; upload.py with HTTP POST and error handling.	Encoder feedback and position verification; Pelco-D Query Pan/Tilt response parsing.
Week 6 (3/31)	Camera feed display module; live video streaming integration into web dashboard.	toplevel1.py campaign orchestrator daemon: spawn final.c with parsed protocol parameters.	final.c C program development: VNA SCPI control and nested-loop measurement state machine.
Week 7 (4/7)	Real-time S-parameter data plotting with Chart.js; frequency response graphs for S11 and S21.	toplevel2.py data post-processor daemon; trans.py log-to-CSV parser development.	Camera hardware mounting on modified drying rack with rotation mechanism; initial field testing.
Week 8 (4/14)	3D Digital Twin model rendering; antenna pose real-time synchronization with measurement data.	Full pipeline integration testing: protocol download to measurement execution to data upload.	PCB design and fabrication: touch-sensitive LED strip circuit; 3D-printed housing design.
Week 9 (4/21)	Accuracy testing: angle positioning verification (+/-1 degree); data display validation.	Cloud platform reliability testing; 100-cycle bidirectional communication stress test.	PCB assembly and ladder mounting; touch-sensing calibration and nighttime visibility test.
Week 10 (4/28)	System integration and debugging; end-to-end unattended measurement campaign test.	System integration and debugging; error handling for network interruptions and retry logic.	System integration and debugging; PTZ + VNA coordinated operation and timing tuning.
Week 11 (5/5)	Performance testing: video stream latency measurement, communication reliability validation.	Performance testing: data upload success rate, protocol detection latency (target < 3s).	System-level validation; power sequencing test; auto-shutdown verification; wind load analysis.
Week 12 (5/12)	Final presentation preparation; demo video recording and editing.	Final report writing: Automation Control System and Cloud Communication sections.	Final report writing: Rotation Control, Power System, and Environmental Protection sections.

4 Requirements & Verification

This section outlines the requirements of our design, the verification procedures we used to test them, and the quantitative results achieved.

4.1 Scatterometer Measurement Subsystem (SMS) Requirements

Table 4.1 Scatterometer Measurement Subsystem Requirements and Verification

#	Requirement	Verification Process	Result
SMS-1	Upon receiving a target angle step pair (HRS, VRS), the scatterometer shall automatically execute a grid scan sequence, designating (HRS, VRS) as the terminal point of the measurement path.	Initialize a scan command with a specific target coordinate, e.g., (30°, 40°). Monitor the instrument and the log messages to track the real-time trajectory. Confirm the terminal coordinate.	Passed. The system executed a systematic grid pattern and successfully terminated at the exact input (HRS, VRS) coordinates.
SMS-2	The scatterometer must support a user-defined "Auto-Shutdown" toggle to be executed immediately following the conclusion of data acquisition.	Send a measurement command with the “Auto-Shutdown” flag set to True. Observe the instrument status after the final data point is recorded. Repeat the test with the False flag to verify the idle state.	Passed. The machine initiated a safe shutdown sequence upon scan completion when True, and remained in standby when False.
SMS-3	The subsystem shall locally log S11, S21, frequency, and both terminal and real-time scanning angles for each measurement point.	Execute a sample grid scan. Verify that every data row in the generated file contains the needed fields: S11, S21, Frequency, Target Angles, and Current Angles.	Passed. Local logs were generated automatically with all parameters required recorded.
SMS-4	The robotic assistant shall execute smooth multi-axis movements with an angular positioning resolution of at least 1°.	Command the robotic joint to move to specific angular targets, e.g., 30°. Measure the actual mechanical displacement.	Passed. The recorded positioning deviation was within ±0.15°.

4.2 Interactive Visualization Subsystem (IVS) Requirements

Table 4.2 Interactive Visualization Subsystem Requirements and Verification

#	Requirement	Verification Process	Result
IVS-1	The interactive command interface shall register and transmit a set of user commands to the cloud within 500ms after the user clicks the button. The command set shall include horizontal and vertical rotation angles (0°-180°, multiple of 10) and a toggle for the post-measurement power state.	Input a comment set, e.g., (30, 40, Yes) and click the "Start Measurement" button. Check the command data in the cloud database. Use internal logs of the cloud server to measure time latency.	Passed. Commands were successfully uploaded to the cloud database at 100ms to 350ms. Validated that only multiples of 10° between 0° and 180° were accepted.
IVS-2	The data interface should fetch the latest data from cloud storage in real time, with a time lag of no more than 1s.	Manually upload a data file to the cloud database. Measure the data fetch process using synchronized system clocks.	Passed. The data interface updated the display within 500ms upon the data upload.
IVS-3	The data interface should correctly plot the graph showing the frequency response of the S11 and S21 from the cloud data, with a time lag of no more than 5s.	Manually upload a data file to the cloud database. Compare the UI-generated plot with a reference plot generated by Excel.	Passed. The UI accurately plotted the frequency response of the input S11 and S21 within an average of approximately 3s.
IVS-4	The data interface shall provide a data download function allowing the user to retrieve and save cloud-stored measurement logs in .txt format, and a data clearance function enabling the user to delete stored records to prepare for a new measurement sequence.	Click "Download Data" and verify the exported file. Click "Clear Data" and verify the could database and UI display.	Passed. Files were able to be exported and were consistent with the cloud database. The cloud database was able to be cleared.
IVS-5	The user interface shall inform the user of task completion immediately after the final data point of a scan is logged, with a time lag of no more than 100ms.	Launch a full scan sequence. Verify that a "Measurement Complete" notification appears instantly once the terminal coordinate is logged.	Passed. The UI triggered a completion notification immediately after receiving the final data packet within 50ms.
IVS-6	The 3D model should reflect the scatterometer's state	Compare the rotation of the 3D model with the	Passed. The 3D model orientation matched the

	corresponding to the latest returned data in real time, with a time lag of no more than 100ms; the horizontal and vertical rotation angles should match the returned data.	current angles returned from the cloud. Verify visual alignment at various angels.	measurement data with no perceptible lag. Angular movements were consistent with the returned data.

4.3 Remote Communication Subsystem (RCS) Requirements

Table 4.3 Remote Communication Requirements and Verification

#	Requirement	Verification Process	Result
RCS-1	The subsystem shall synchronize commands from the cloud to the local computer in real-time, with a maximum allowable transmission latency of 1s.	Send a series of 100 test commands from the cloud and calculate the duration until local reception.	Passed. The average transmission latency was recorded at 100ms to 350ms under standard network conditions, well within the 1s limit.
RCS-2	The subsystem shall automatically synchronize the locally stored measurement data to the cloud database immediately upon file generation, with a maximum allowable upload latency of 1s.	Trigger a measurement scan. Record the file creation time on the local PC and compare it with the data receipt timestamp in the cloud database.	Files were synchronized immediately upon generation. The maximum observed upload latency was 500ms for a full scan dataset, well within the 1s limit.
RCS-3	The cloud infrastructure must provide sufficient storage to accommodate the complete dataset resulting from a maximum-range grid scan (180°×180°) without data loss or overflow.	Perform a theoretical calculation of the data volume for a 180×180 grid. Upload a simulated dataset of the same size to the cloud and verify data integrity.	The cloud database successfully ingested the entire set without overflow, and no data packets were dropped during the test.

4.4 Ladder Lighting Subsystem (LLS) Requirements

Table 4.4 Ladder Lighting Subsystem Requirements and Verification

#	Requirement	Verification Process	Result
LLS-1	The touch-sensitive interface on the ladder frame shall allow	Touch the designated sensor area on the ladder frame and observe the LED state.	Passed. The touch interface responded instantaneously to direct skin contact, successfully

	users to manually turn on or off the LED through direct skin contact.	Repeat the contact to test the toggle-off logic. Conduct 50 cycles to check stability.	toggling the illumination state between On and Off without false triggers or dead zones.
LLS-3	The power should integrate a DC-DC boost converter to step up the battery voltage (3.7V) to a regulated 5V output for the 4.8W LED array.	Measure the output voltage of the boost converter using a digital multimeter under maimum load (4.8W) while the battery discharges from full to depleted.	Passed. The boost converter maintained a stable 5.01V ±50mV output across the discharge cycle.
LLS-4	The onboard charging circuit shall restrict the charging current to 400mA via a USB-C interface.	Connect the depleted system to a 5V USB-C power source and series ammeter. Record the charging current profile and total time to reach full charge.	Passed. Charging current was regulated at approximately 396mA. The full chage cycle finished successfully in approximately 1.25 hours without overheating.

4.5 Monitoring Subsystem (MS) Requirements

Table 4.5 Monitoring Subsystem Requirements and Verification

#	Requirement	Verification Process	Result
MS-1	The video feed shall be High-Definition (HD) to provide sufficient visual clarity for users to discern the precise rotation angles of at least 10°.	Rotate the scatterometer in increments of 10°. Verify that an observer can clearly recognize and visually distinguish each individual step change via the monitor.	Passed. The 5-megapixel camera provided excellent spatial resolution. Every 10° rotation was clearly identifiable on the UI without blurring or pixelation.

4.6 Requirement Verification Summary

The verification process confirms that the system meets all functional and performance requirements with high-efficiency timing and synchronization across all subsystems, acheiving the objective of digital twin. As illustrated in Figure 4.6, the time for a command to transfer from the user interface through the command cloud server to the scatterometer was between 200ms to 700ms in total. Measurement data upload from the scatterometer to the database remained highly efficient with a latency of less than 500ms. The end-to-end delay for measurement data processing and plotting on the user interface was verified at under 3s.

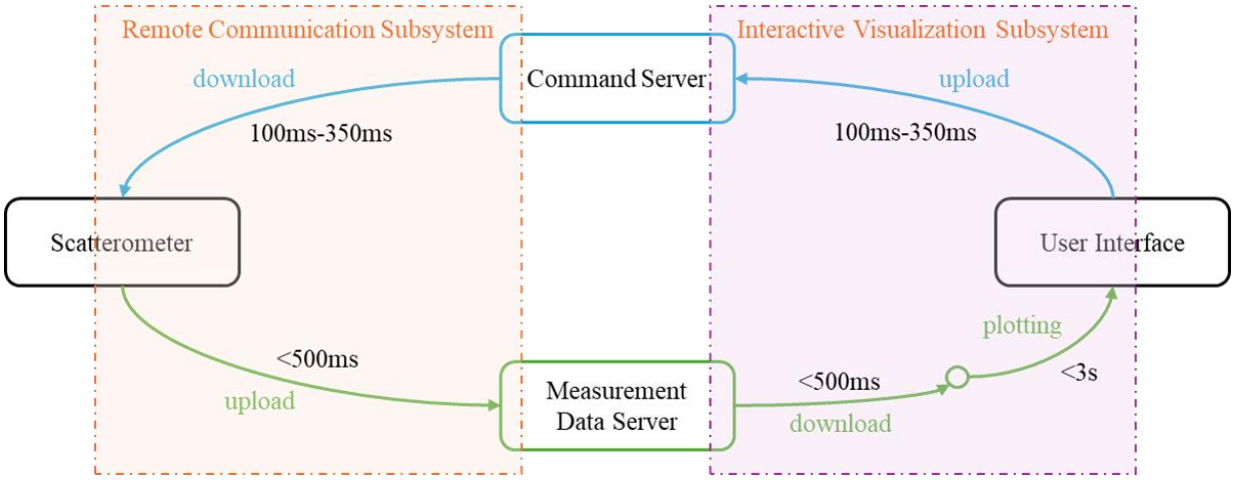

Figure 9: Block diagram of remote communication subsystem and interactive visualization subsystem showing latency.

Furthermore, the monitoring subsystem successfully maintained a real-time clear video feed with minimal lag. The ladder lighting subsystem and scatterometer measurement subsystem demonstrated robust stability, with the latter successfully executing automated grid scans and power-management sequences.

5 Conclusion

This report has presented the complete design, implementation, and experimental validation of an automated microwave scatterometer system with an integrated cloud-based digital twin. The project demonstrates a work Communing cyber-physical measurement pipeline that bridges hardware instrumentation—a dual-axis PTZ antenna positioner and a vector network analyzer—with cloud services for command dispatch, data archival, and interactive visualization. The system achieves the core project objective: enabling fully unattended microwave scattering measurements over programmable angular grids for soil characterization applications.

5.1 Accomplishments

Our project achieved all primary objectives and delivered several key results:

1.End-to-End Measurement Automation: We developed a complete automation pipeline that coordinates PTZ antenna positioning, VNA S-parameter acquisition, cloud protocol download, and automated data upload without human intervention. The system executes a full 10×10 angular grid (100 measurement positions, 200 S-parameter sweeps) autonomously, compared to hundreds of manual positioning and recording operations in the conventional workflow.

2.Cloud-Connected Digital Twin: We implemented a bidirectional cyber-physical architecture using a dual Render platform deployment. The Command Server dispatches measurement protocols and the Data Server archives results. A web-based interactive interface combines a control panel, S-parameter data dashboard, and 3D digital twin view with real-time antenna pose synchronization, enabling remote operation and visualization.

3.Broadband S-Parameter Acquisition: The VNA measurement subsystem successfully acquires S11 and S21 magnitude across the 5–8 GHz C-band at 25 frequency points per sweep. All data is archived in per-angle timestamped log files, providing a complete and traceable measurement record for each campaign.

4.Remote Monitoring and Safety: An HD camera provides live video streaming with sub-1-second latency for remote instrument status observation. A custom touch-sensitive LED strip PCB, enclosed in a 3D-printed housing and mounted on the support ladder, provides on-demand illumination for nighttime operator safety.

5.2 Uncertainties and Challenges

While the system met all core requirements, several challenges and sources of uncertainty were identified:

1.Phase Measurement Anomaly: The phase data consistently recorded 0.000° for both S11 and S21 across all frequency points and angular positions. This indicates a VNA configuration or calibration issue rather than a physical phenomenon. This limits the current system's utility for complex permittivity retrieval.

2.Single-Point Software Failures: The two Python controller daemons (toplevel1.py and toplevel2.py) each run as single processes without supervisory monitoring. A crash in either

process silently halts the corresponding portion of the measurement pipeline. The current system lacks a watchdog mechanism to detect and restart failed daemons.

3.VNA Timing Variability: The VNA SCPI command processing latency exhibited non-deterministic variation. Occasional anomalous delays exceeding 10 seconds were observed. The root cause—whether VNA firmware scheduling, USB-to-TCP bridge latency, or RF front-end settling—has not been definitively isolated.

5.3 Future Work

Based on our development experience and testing results, we identify several directions for future enhancement:

1.VNA Calibration and Phase Recovery: The highest-priority improvement is implementing a full two-port SOLT(Short-Open-Load-Through) or electronic calibration routine integrated into the automated measurement sequence. Correcting the phase measurement anomaly would unlock complex S-parameter capability required for dielectric permittivity inversion.

2.Multi-Frequency Extension: Extending frequency coverage to include L-band (1–2 GHz) and X-band (8–12 GHz) would enablemmulti-frequency soil moisture retrieval algorithms that exploit different penetration depths and scattering mechanisms at each band.

3.Integrated Environmental Sensing: Adding in-situ sensors such as soil moisture probe, soil temperature thermocouple, air temperature sensor, and anemometer would enable direct correlation between S-parameters and ground-truth environmental conditions.

4.Software Reliability Hardening: The Python daemons should be wrapped as Windows Services with automatic restart on failure. A dedicated watchdog process should monitor daemon health and log anomalies. Structured JSON-format logging would facilitate post-hoc debugging of field issues.

5.4 Ethical Considerations

The design, development, and intended use of this system are consistent with the IEEE Code of Ethics and responsible engineering practice. The scatterometer operates in the 5–8 GHz C-band with conducted RF power below +10 dBm directed at the soil surface at near-nadir angles, presenting no hazardous RF exposure under FCC and ICNIRP guidelines. The auto-shutdown feature supports energy conservation, and unattended operation reduces the carbon footprint associated with personnel travel to remote field sites. All measurement data is archived with full provenance in open, documented formats (CSV, plain text) using vendor-independent protocols (Pelco-D, VISA/SCPI, HTTP REST) to ensure accessibility, auditability, and reproducibility. The system is configured exclusively for downward-looking soil scatterometry, with mechanical range limits and power levels that constrain it to its intended environmental sensing purpose. No human subjects, personally identifiable information, or privacy-sensitive data are involved in any workflow. This project was conducted as part of the ECE 445 Senior Design Laboratory curriculum at the Zhejiang University–University of Illinois Urbana-Champaign (ZJUI) Institute, with all work performed by the listed team members.

References

[1] J. G. Hofste, R. van der Velde, X. Wang, D. Zheng, J. Wen, C. van der Tol, and Z. Su, "Year-long, broad-band, microwave backscatter observations of an alpine meadow over the Tibetan Plateau with a ground-based scatterometer," Earth System Science Data, vol. 13, no. 6, pp. 2819–2856, 2021, doi: 10.5194/essd-13-2819-2021.

[2] A. Fuller, Z. Fan, C. Day, and C. Barlow, "Digital twin: Enabling technologies, challenges and open research," IEEE Access, vol. 8, pp. 108952–108971,2020,doi:10.1109/ACCESS.2020.2998358.

[3] F. Tao, H. Zhang, A. Liu, and A. Y. C. Nee, "Digital twin in industry: State-of-the-art," IEEE Transactions on Industrial Informatics, vol. 15, no. 4, pp. 2405–2415, 2019, doi: 10.1109/TII.2018.2873186.